



An application of geospatial-based multi-criteria decision-making technique to identify landslide susceptibility zones in the Ragnu Khola River Basin of Darjeeling Himalayan region, India

Dipesh Roy¹ · Satyajit Das¹ · Rajib Mitra¹

Received: 27 January 2022 / Accepted: 18 September 2022 / Published online: 26 September 2022
© The Author(s), under exclusive licence to Società Italiana di Fotogrammetria e Topografia (SIFET) 2022

Abstract

One of the most dangerous geo-hazards, landslides cause a progressive loss of rock and soil that have a negative impact on human lives, the ecosystem, and the global economy. Darjeeling Himalaya is one of the world's young fold mountainous areas, often suffering from landslide hazards. Hence, the study identifies the landslide susceptibility zone in the Ragnu Khola River Basin of the Darjeeling Himalayan region by applying the geospatial-based MCDM technique. This research's major goal is to identify whether this GIS-based multi-criteria decision-making (MCDM) technique is validated or not for landslide susceptibility zones (LSZ); if validated, then how much manifests for describing the LSZ in the study area. MCDM evaluation applies to determining weight value to integrate different thematic layers of river morphometry like drainage diversity (DD) parameters and relief diversity (RD) parameters. Both DD and RD have significant impacts on landslide intensity. Hence, both layers are combined using the analytical hierarchy process (AHP) of the MCDM technique for the final LSZ. The final result has been validated by ROC analysis using landslide occurring point data obtained from the Geological Survey of India (GSI). The outcome of the study shows that 1.45% and 17.83% of areas of the region fall in “very high” and “high” LSZ, which belongs to near Mull Gaon, Sanchal forest, and Alubri basti. Most of the area (47.70%) is observed in “moderate” LSZ. Only 1.32% and 31.7% are kept in “very low” and “low” LSZ, respectively, throughout the study area. The description capability of the technique for LSZ is significant as the area under the curve (AUC) is 72.10%. The validation of the study using the frequency density of the landslides (FDL) also indicates the “very high” LSZ is associated with the maximum (2.19/km²) FDL. The work will be necessary to develop the overall socio-economic condition of such kind of tectonically sensitive region through proper and effective planning.

Keywords Landslide susceptibility zones (LSZ) · River morphometry · MCDM technique · ROC-AUC

Introduction

A natural hazard is an extreme occurrence that harms humans or other things that we care about (White 1974). In mountainous regions, many natural hazards can happen in the form of landslides, avalanches, debris flows, and

flash floods. Among them, landslides are the most common (Pourghasemi et al. 2012b). The saturation of soil and erosion of rock by water increased due to high rainfall, reduced plant cover, and rapid urban growth in the hilly areas. As a result, landslides occur on high gradient slopes in mountain areas (Chamling 2013; Bhattacharya 2013; Nad 2015). The occurrences of landslides are directly caused risks to human beings and losses in private and public assets (Petley 2012; Pourghasemi et al. 2012b). However, a study from 1964 to 1999 revealed that there is a positive increase in the number of landslide events happening around the world (Nadim and Kjekstad 2009). From 1990 to 2005, it accounted for 4.89% of all-natural disasters globally (Alano and Lee 2016; Islam and Khan 2018). Landslide susceptibility zones (LSZ) must be identified before landslide mitigation measures may be implemented (Varnes 1984).

✉ Dipesh Roy
dipeshroy47@gmail.com
Satyajit Das
dassatyajit458@gmail.com
Rajib Mitra
rajibmitrageo@gmail.com

¹ Department of Geography and Applied Geography,
University of North Bengal, Siliguri, West Bengal, India

Landslides are the most widespread disaster in the Darjeeling Himalayan region. It is one of the world's young fold mountainous regions. Climatic variability, tectonic disturbances, geological properties, and increased anthropogenic activity such as road, building, and resort construction have integrated caused landslides in various regions of the Darjeeling Himalaya (Basu and Pal 2018). Landslide susceptibility studies in the Darjeeling Himalayas are found in the work of Bhattacharya (2013), Chawla et al. (2018), Chakraborty et al. (2018), Mandal and Mandal (2018), Das and Lepcha (2019), Saha and Saha (2021), Das et al. (2022). According to the expert opinion, several previous studies on landslide susceptibility mapping (LSM) were done based on manual interpretations of various thematic layers (Sarkar et al. 1995; Virdi et al. 1997). Researchers have used quantitative approaches in contemporary periods, viz. artificial neural networks (Moayedi et al. 2019a, b; Lucchese et al. 2021a, b; Jacinth Jennifer and Saravanan 2021; Mehrabi and Moayedi 2021), logistic regression analysis (Gu et al. 2021; Crawford et al. 2021; Sujatha and Sridhar 2021), fuzzy logic (Bahrami et al. 2021; Manaouch et al. 2021; Nanehkaran et al. 2021), multivariate regression analysis (Arabameri et al. 2019; Chu et al. 2019; Pham et al. 2021), and bivariate regression analysis (Zhou et al. 2021) to delineate LSZ. Machine learning approaches are now widely used to predict natural disasters such as floods, wildfires, earthquakes, and droughtiness, among others (Hong et al. 2018; Ahmadlou et al. 2019; Mehrabi 2021).

Now, this study uses a multiple-criteria decision-making (MCDM) approach from remotely sensed data to emphasize the need to create the thematic layers of landslide trigger factors that account for the zonation of possible landslide hazard zones (Saha et al. 2002, Sarkar and Kanungo 2004). Morphology is the measurement and quantitative investigation of the earth's surface and landforms (Clarke 1996; Agarwal 1998; Reddy et al. 2004). To understand the hydro-geological properties, morphometric analysis is essential. It also expresses the prevailing climatic, topographic, geological, and geomorphological conditions of the concerned area (Horton 1945; Strahler 1952; Hurtrez et al. 1999; Basu and Pal 2018).

The study has been conducted using morphometric variables to demonstrate the LSM of the Ragnu Khola River Basin in the Darjeeling Himalayan region. To achieve the goal, a large number of morphometric variables were taken into account. The two broad aspects of morphometric analysis used to identify LSZ, viz. drainage diversity (DD) and relief diversity (RD) (Pal and Saha 2017; Basu and Pal 2018; Basu and Pal 2019). In the present study, the authors have used the analytical hierarchy process (AHP) for the weight generation of different landslide susceptibility indicators. The AHP is a widely used strong MCDM technique for weighting the indicators (Navarro et al. 2019; Kaur et al.

2020; Zarei et al. 2021), as postulated by Saaty (Saaty 2004, 2008). An attempt to check the final output map is also made during the accuracy assessment. The work's novelty lies in the utilization of morphometric techniques with the integration of the AHP method in the studied region. There is no published systematic and scientific research based on the landslide susceptibility mapping of this study area. The work is original, and this kind of study has not already been found in this area. Therefore, the authors found the research gaps in this landslide-prone river basin in the Darjeeling Himalayan region and selected it for the current study. The outcome of the work will aid government agencies, policymakers, and planners in reducing landslide-related damages and proper planning for land use in the areas with "very high" landslide susceptibility of the Ragnu Khola River Basin.

Materials and methods

Study area

The Ragnu Khola River basin, considered the study area, is located in the Darjeeling district of West Bengal in India. The latitudinal extension of this river basin is from 27° 00' 19" N to 27° 06' 30" N, the longitudinal extension is from 88° 16' 03" E to 88° 21' 21" E, and the basin area is about 64.79 km². The river Ragnu Khola is also known as the Rongdong River. It is a very small river basin originating from the eastern down part of Darjeeling town. The drainage pattern of this river basin is the dendritic type which means that the river basin has structural control. The Ragnu Khola River finally meets with the Bari Rangit River, which is the major tributary of the Tista River. This river flows in the north-eastern direction based on the natural slope of the region. The basin elevation ranges from 230 to 2478 m, and most of the area is rocky type. The climatic condition of this river basin is monsoon type, and most of the rainfall happens during this monsoon period. The average annual rainfall of the region is approximately 3094.40 mm. In summer, the maximum temperature is about 26 °C, while the minimum temperature is about 19 °C. But in the winter season, it remains very low such as the maximum temperature is about 6 °C and the minimum temperature is –2 °C (District Survey Report 2021; Climate-Data.Org 2021). Most of the landslides occur during the rainy season when heavy rainfall occurs in a short period. Figure 1 depicts the location map of the study area with the spatial distribution of historical landslide sites within the basin.

Data acquisition and methods for LSM

For extracting the stream network of the Ragnu Khola River Basin, a toposheet has been collected from the

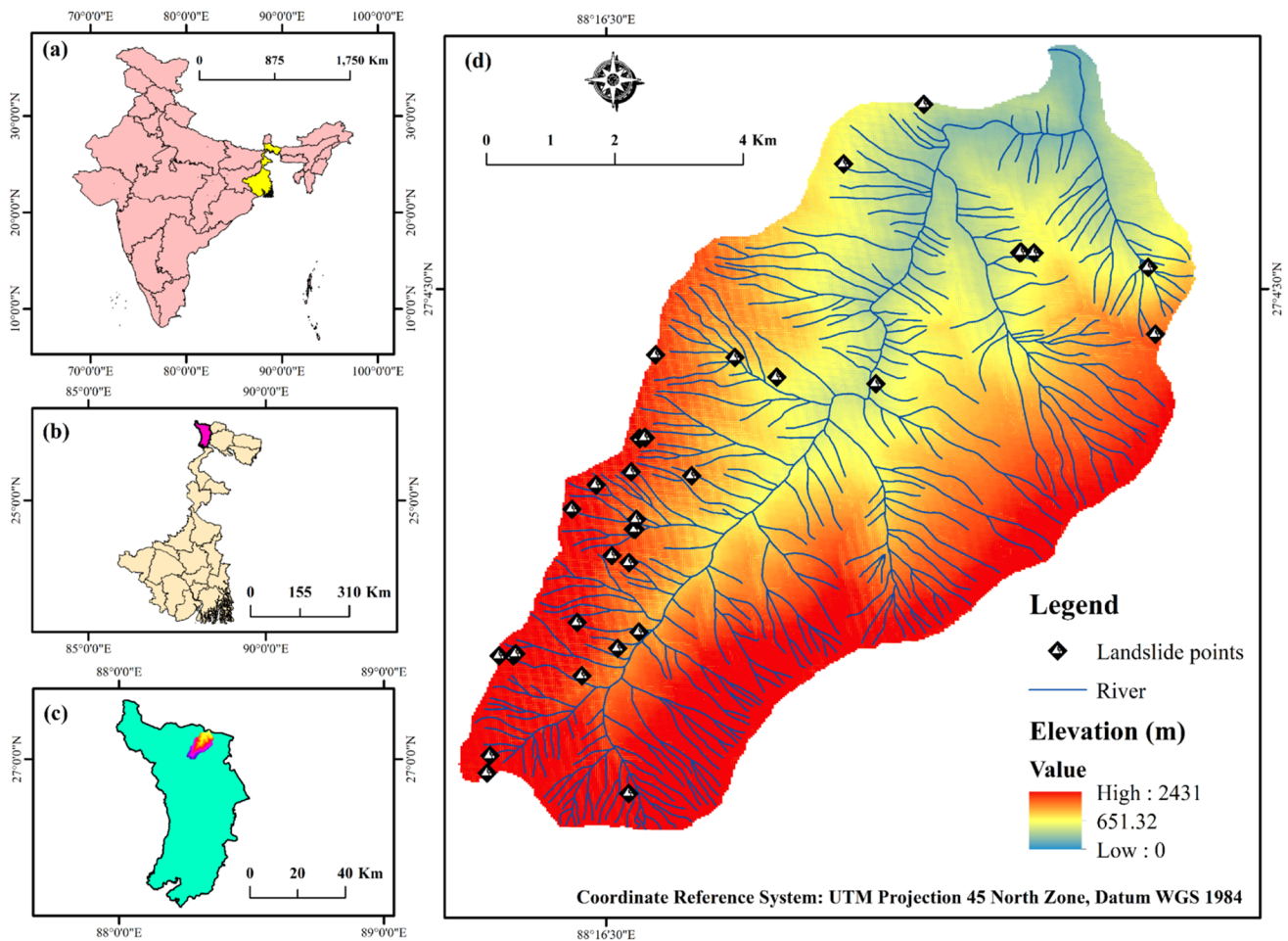


Fig. 1 a India, b West Bengal, c Darjeeling district, and d Ragnu Khola River Basin in the Darjeeling Himalaya with landslide occurrence points

Survey of India (SOI). The topographical map has the G45E8 number on a 1:50,000 scale. The map was geo-referenced using ArcGIS software in the UTM projection 45 north zone, with datum WGS 1984, and all stream networks of the study area were digitized. Along with this, the researchers also used SRTM DEM (30 m) to delineate the basin with the help of the ArcGIS “hydrology” tool. The necessary data and maps are also collected from the different government websites. The acquired datasets are mentioned in Table 1, and the methodological framework of the work is shown in Fig. 2. The essential part of delineating LSM is the selection of appropriate landslide conditioning indicators. Hence, the present study was considered based on the frequent landslide occurring factors used in several studies (Arabameri et al. 2017; Saleem et al. 2019; Liu et al. 2021). Here, 16 indicators are taken as landslide conditioning indicators, categorized into two broad groups: relief diversity (RD) and drainage diversity (DD). A detailed description of the RD and DD indicators is given below:

Relief diversity indicators

The basin elevation (Be) is vital in landslide conditioning indicators as its gravitational potential energy (Chen et al. 2019). Variation in elevation of any region affects the geomorphological features, nature of the vegetation, and degree of erosion. Thus, changes in elevation influence landslide susceptibility (Chen et al. 2017). The relief map of the region is depicted in Fig. 3a. The slope (SI) is considered the most significant indicator for mapping landslide susceptibility. It can be used to know the steepness of the topography (Chen et al. 2019), and it has a direct influence on occurrences of landslides. The “SI” map has been prepared from SRTM DEM (30 m resolution). The basin exhibits a variety in “SI,” ranging from 0.33 to 59.42°, as displayed in Fig. 3b. As a topographic indicator, the aspect (As) affected the landslides, which are triggered due to rainfall (Beullens et al. 2014; Gorokhovich and Vustianiuk 2021). It is referred to as the direction of the slope of any region. It is interrelated with the microclimatic parameters and azimuth of the flow

Table 1 Data used and their sources to identify LSZ in the Ragnu Khola River Basin

Data	Parameters	Symbol	Source	Resolution	Classification method
Topographical map	Dissection index	Di	Survey of India (SOI) https://soinakshe.uk.gov.in/	30*30	Natural break (Moayed et al. 2019a, b)
	Ruggedness index	Ri	SOI https://soinakshe.uk.gov.in/	30*30	Natural break (Moayed et al. 2019a, b)
	Relative relief	Rr	SOI https://soinakshe.uk.gov.in/	30*30	Natural break (Moayed et al. 2019a, b)
	Basin elevation	Be	SOI https://soinakshe.uk.gov.in/	30*30	Natural break (Moayed et al. 2019a, b)
	Stream frequency	Fs	SOI https://soinakshe.uk.gov.in/	30*30	Natural break Moayed et al. 2019a, b)
	Drainage density	Dd	SOI https://soinakshe.uk.gov.in/	30*30	Natural break Moayed et al. 2019a, b)
	Length of overland flow	Lo	SOI https://soinakshe.uk.gov.in/	30*30	Natural break Moayed et al. 2019a, b)
	Drainage texture	Dt	SOI https://soinakshe.uk.gov.in/	30*30	Natural break Moayed et al. 2019a, b)
	Junction frequency	Jf	SOI https://soinakshe.uk.gov.in/	30*30	Natural break Moayed et al. 2019a, b)
	Infiltration number	In	SOI https://soinakshe.uk.gov.in/	30*30	Natural break Moayed et al. 2019a, b)
ASTER DEM	Slope	Sl	United States Geological Survey (USGS) https://earthexplorer.usgs.gov/	30*30	Natural break Moayed et al. 2019a, b)
	Aspect	As	USGS https://earthexplorer.usgs.gov/	30*30	Natural break Moayed et al. 2019a, b)
Geological map	Lithology	Lg	Geological Survey of India (GSI) https://www.gsi.gov.in/	30*30	Lithological units
	Lineament density	Ld	GSI https://www.gsi.gov.in/	30*30	Natural break Moayed et al. 2019a, b)
Soil map	Soil type	St	National Bureau of Soil Survey and Land Use Planning (NBSS and LUP) https://www.nbsslup.in	30*30	Textural units

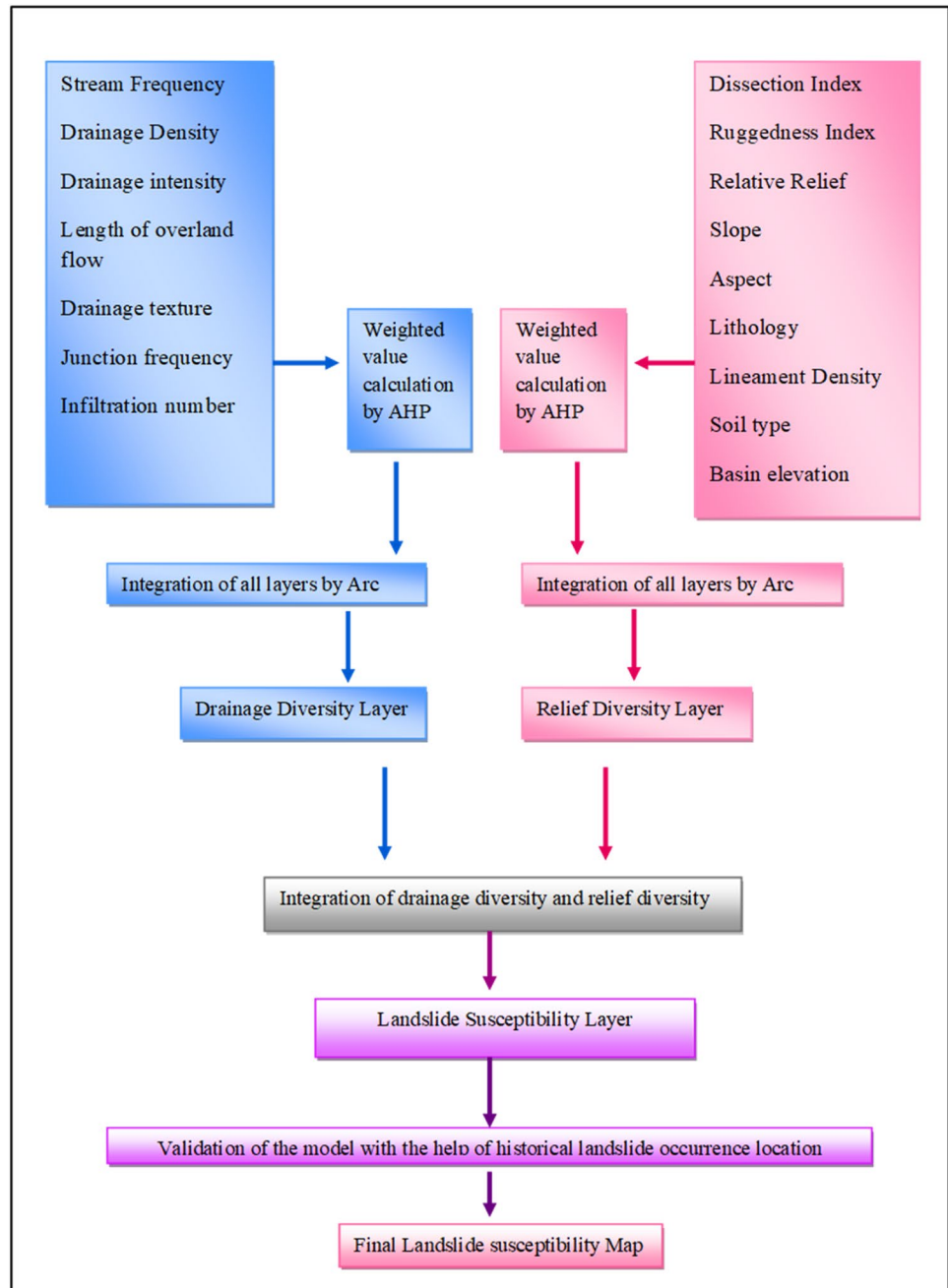
(Erener and Düzgün 2010; Mondal and Mandal 2019). It also affects the variation in temperature, relative humidity, and vegetation coverage of a slope (Bennie et al. 2006). The “As” map of the study area is depicted in Fig. 3c. The landslide susceptibility mapping is interrelated with the lithological properties of that area (Pourghasemi et al. 2012a; Mandal and Maiti 2014). The rock strength and permeability of the land surface vary as per the lithological formations (Ayalew and Yamagishi 2005; Wang et al. 2020). The lithological data has been obtained from the Geological Survey of India (GSI). It manifested that three formations are present in the basin, i.e., Gorubathan, Kanchenjunga Gneiss, and Chungthang, as displayed in Fig. 3d. Most of the part of the basin is covered with the Kanchenjunga Gneiss formation. The ruggedness index (Ri) is used to understand the instability and structural complexity of the topography (Strahler 1956; Schumm 1956). The basin demonstrates the range of “Ri” is from 0 to 3.12 (Fig. 3e). It was computed using Eq. 1, where *Rr* stands for relative relief, *Dd* stands

for drainage density, and *K* stands for constant (Patton and Baker 1976).

$$Ri = \frac{Rr \times Dd}{K} \quad (1)$$

The presence of lineaments in any area directly influences landslide susceptibility (Keefer and Larsen 2007; Kaur et al. 2018). Hence, it has been taken as an essential landslide conditioning indicator. It represents the geomorphologic signatures like topographic breaks, shear zones, tectonic structures, and discontinuities (Sarkar and Kanungo 2004; Ayalew and Yamagishi 2005). The lineament density (Ld) map of the basin is represented using the “line density” tool in ArcGIS. The “Ld” value ranges from 0 to 1.83 km/km² (Fig. 3f). The Higher “Ld” region has a high probability of frequent landslides (Erener and Düzgün 2010). Soil is an essential indicator for mapping landslides susceptibility because shallow depth soils are mostly affected during landslides (Sharma et al. 2012).

Fig. 2 Methodological framework of the present study



In the study area, two soil classes are identified (Fig. 3g) from the soil map of the NBSS and LUP. The classes are “W002” (coarse loamy) and “W004” (loamy-skeletal). Both soils are moderately shallow in-depth, and well-drained. “W002” soil is associated with strong rockiness and severe erosion, while “W004” soil has moderate rockiness and moderate erosion. Relative relief (Rr) is the difference in the highest and lowest altitude of a unit area. It is also known as “amplitude of relief” or “local relief” (Iqbal et al. 2021). It helps to analyze the morphological properties of the topography (Gayen et al. 2013; Basu and Pal 2019). The “Rr” map of the study area is prepared

using Eq. 1 by applying the grid method and the “IDW” tool in ArcGIS. The basin represents the “Rr” value varies from 140 to 895 m (Fig. 3h). The formula of “Rr” is as follows (Smith 1935):

$$Rr = H - h, \tag{2}$$

where, *H* is the highest altitude, and *h* is the lowest altitude of a unit area. The high “Rr” zone is associated with landslide susceptible zones (Das and Lepcha2019). Dissection index (Di) is one of the landslide conditioning parameters and has been considered by several researchers (Altın

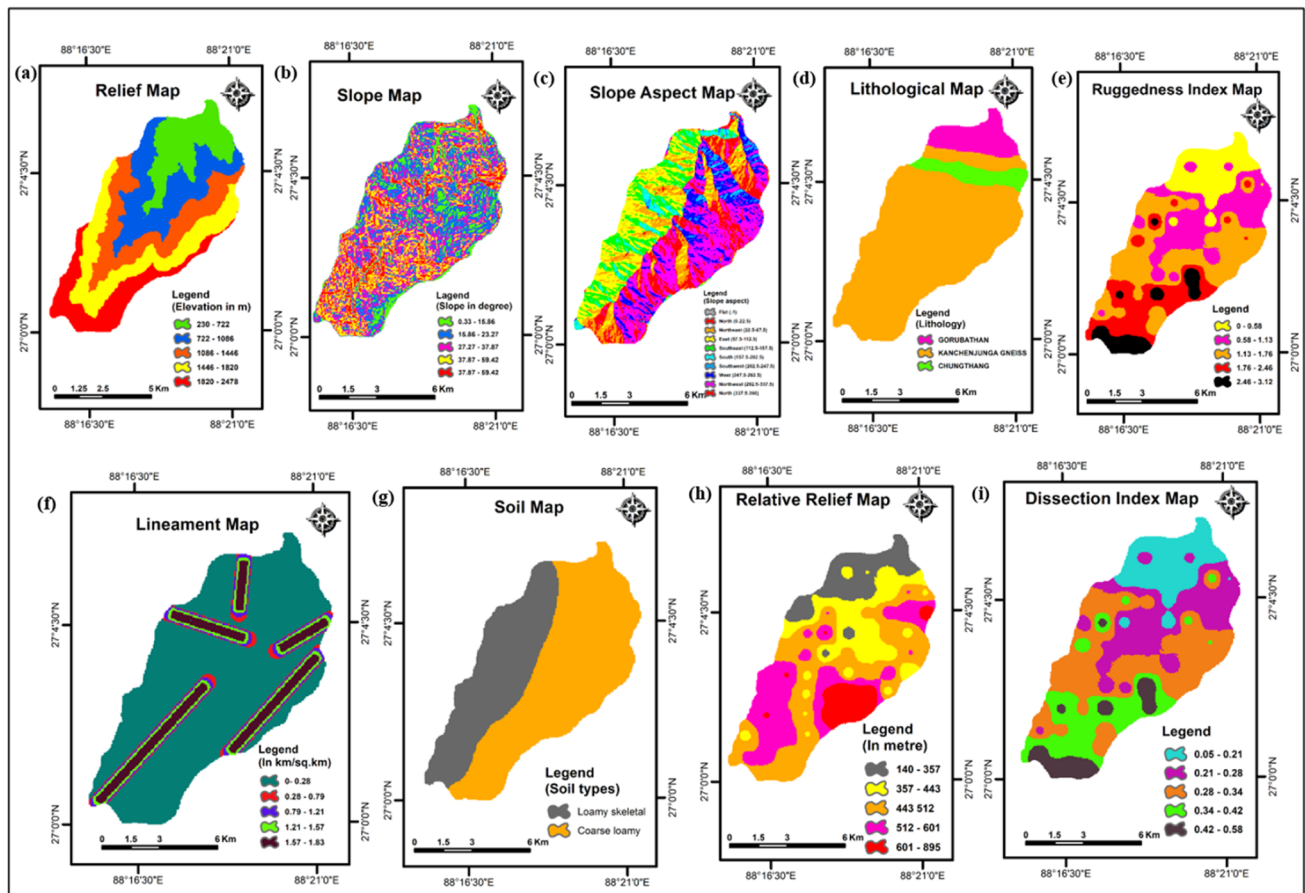


Fig. 3 Raster maps of different relief diversity parameters. **a** Basin relief, **b** slope, **c** slope aspect, **d** lithological formation, **e** ruggedness index, **f** lineament density, **g** soil type, **h** relative relief, and **i** dissection index of the Ragnu Khola River Basin in the Darjeeling Himalaya

and Gökaya 2018; Basu and Pal 2019; Das and Lepcha 2019). “Di” is known as the ratio between relative relief and absolute altitude (Nir 1957). It shows the stage of the landscape development and dissection of the river basin (Altın and Gökaya 2018; Basu and Pal 2019). The study area reflects the “Di” value which varies from 0.05 to 0.58 (Fig. 3i). The regions with high and very high “Di” values are related to the steep sloping lands and high landslide susceptible zone.

Drainage diversity indicators

Drainage density (Dd) is used in the study as the drainage diversity (DD) parameter. “Dd” is one of the prominent landslide conditioning indicators (Sahana and Sajjad 2017). It can be defined as follows (Strahler 1964):

$$Dd = \frac{L\mu}{A} \quad (3)$$

where, $L\mu$ denotes the total length of the river, and A denotes the area drained. The higher “Dd” areas are

mainly associated with the regions with slope failure; hence, it causes landslide phenomena in the hilly watershed (Hasegawa et al. 2014). The value of “Dd” in the study area ranges from 1.84 to 7.15 km/km² (Fig. 4a). The factor stream frequency (F_s) has a direct relationship with the landslides. In this region, “ F_s ” varies from 3 to 24 streams/km², as illustrated in Fig. 4b. The higher “ F_s ” implies higher chances of landslides and vice versa. For the present study, “ F_s ” is computed using Eq. 4, as follows:

$$F_s = \frac{N\mu}{A} \quad (4)$$

where $N\mu$ represents the total number of rivers, and A represents the area (Horton 1945). Drainage intensity (DI) is expressed as the ratio between stream frequency and drainage density (Faniran 1968). It represents the runoff characteristics of any region (Basu and Pal, 2019). Here, “DI” ranges from 0.64 to 5.85, as depicted in Fig. 4c. Higher “DI” areas are characterized by maximum possibilities of landslide hazard, while lower “DI” areas are represented with fewer chances (Das and Lepcha

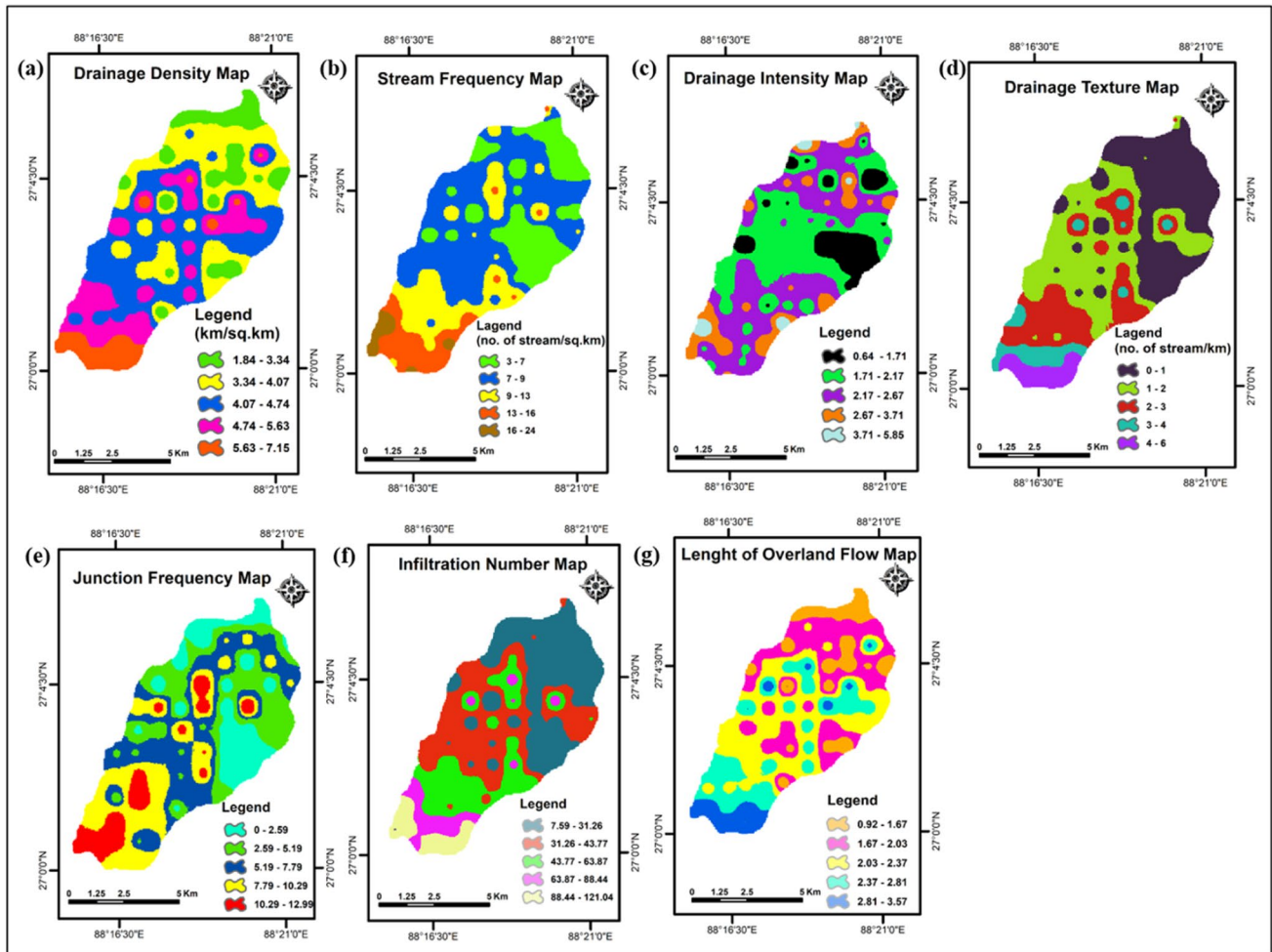


Fig. 4 Raster maps of different drainage diversity parameters. **a** Drainage density, **b** stream frequency, **c** drainage intensity, **d** drainage texture, **e** junction frequency, **f** infiltration number, and **g** length of overland flow of the Ragnu Khola River Basin in the Darjeeling Himalaya

2019). Drainage texture (*Dt*) is associated with the rock, relief, soil, climate, and vegetation characteristics of any region (Kale and Gupta 2001). “*Dt*” can be expressed as follows (Horton 1945):

$$Dt = \frac{N\mu}{P} \tag{5}$$

where, $N\mu$ is depicted as the number of streams, and P is depicted as the perimeter of the basin. The study area has “*Dt*” value from 0 to 6 streams/km (Fig. 4d). The stream junction frequency (*Jf*) is another crucial morphometric parameter of a river basin that influences landslide phenomena. “*Jf*” is defined as the presence of stream junction points in each grid (Das and Lepcha 2019). It indicates the area with an unstable slope; hence, a high “*Jf*” value caused landslides. The “*Jf*” of the region ranges from 0 to 12.99 (Fig. 4e). Infiltration number (*In*) as a morphometric parameter illustrated the runoff intensity and infiltration capacity of the region (Strahler 1964).

The higher “*In*” implies high runoff and low infiltration, and vice versa. The higher rate of infiltration accelerated the movement of landslides (Basu and Pal 2019). The “*In*” is calculated for the present study area using the following equation (Zavoianca 1985):

$$In = Dd \times Fs \tag{6}$$

where, *Dd* represents the drainage density, and *Fs* represents the stream frequency. In the study area, “*In*” varies from 7.59 to 121.04 (Fig. 4f). The length of overland flow (*Lo*) is used as an important morphometric parameter. In terms of hydrologic and physiographic growth, “*Lo*” impacts the drainage basin (Horton 1932). Luo et al. (2015) investigated the influence of “*Lo*” on shallow landslides caused by rainfall. The “*Lo*” is calculated using the following equation (Horton 1945):

$$Lo = \frac{1}{2} \times Dd \tag{7}$$

Table 2 Saaty's (2005) scale of relative importance

Numerical value	Definition
1	Equal importance
2	Equal to moderate importance
3	Moderate importance
4	Moderate to strong importance
5	Strong importance
6	Strong to very strong importance
7	Very strong importance
8	Very to extremely strong importance
9	Extreme importance

where *Dd* is the drainage density. The study area exhibits the “Lo” value ranging from 0.92 to 3.57 km, as depicted in Fig. 4g.

Weight value calculation by AHP

The work primarily focuses on preparing the DD and RD thematic layers. Hence, drainage density (*Dd*), drainage texture (*Dt*), drainage intensity (*DI*), infiltration number (*In*), stream frequency (*Fs*), length of overland flow (*Lo*), and junction frequency (*Jf*) factors were analyzed and combined to create the

DD layer. On the other hand, the relief diversity (*RD*) layer was prepared by the integration of basin elevation (*Be*), soil type (*St*), dissection index (*Di*), ruggedness index (*Ri*), relative relief (*Rr*), slope (*Sl*), aspect (*As*), lithology (*Lg*), and lineament density (*Ld*) parameters (Pal and Saha 2017; Basu and Pal 2018; Basu and Pal 2019). Finally, LSM has been created using AHP techniques by integrating the *RD* and *DD* thematic layers with a 50% weightage value for both in ArcGIS software. The AHP is a one-level scoring process that examines indicators using a pair-wise comparison matrix table (Saaty 1990). A nine-point scale (Table 2) is used to rate each criterion's relative preferences on each basis (Malczewski 2006). The scale was utilized to give a verbal expression to the numerical values that were then employed as computed translations to calculate factor weights for correct mapping. The main objective of the AHP framework is to score the weight of each *LSZ* determining factor. The quality of the outcome was highly discretionary because of the subjective nature of pair-wise comparisons. Due to several paths on which the relative relevance of components was appraised, the level of consistency was employed in making the judgments. The weights of *LSZ* parameters such as “*Dd*,” “*Dt*,” “*DI*,” “*In*,” “*Fs*,” “*Lo*,” “*Jf*,” “*Be*,” “*St*,” “*Di*,” “*Ri*,” “*Rr*,” “*Sl*,” “*As*,” “*Lg*,” and “*Ld*” are summarized in the pair-wise comparison matrix (Table 3 and Table 4). Here, normalized weights were assigned and

Table 3 Pair-wise comparison matrix of nine selected parameters for preparing relief diversity map

	<i>Be</i>	<i>Sl</i>	<i>As</i>	<i>Lg</i>	<i>St</i>	<i>Ld</i>	<i>Rr</i>	<i>Ri</i>	<i>Di</i>	Weight
<i>Be</i>	1.00	0.17	4.00	0.14	0.17	0.17	0.20	1.00	1.00	0.03
<i>Sl</i>	6.00	1.00	9.00	5.00	2.00	5.00	6.00	5.00	6.00	0.32
<i>As</i>	0.25	0.11	1.00	0.20	0.17	0.17	0.20	0.25	0.25	0.01
<i>Lg</i>	7.00	0.20	5.00	1.00	1.00	2.00	4.00	5.00	4.00	0.15
<i>St</i>	6.00	0.50	6.00	1.00	1.00	4.00	5.00	6.00	6.00	0.20
<i>Ld</i>	6.00	0.20	6.00	0.50	0.25	1.00	2.00	4.00	5.00	0.10
<i>Rr</i>	5.00	0.17	5.00	0.25	0.20	0.50	1.00	4.00	4.00	0.08
<i>Ri</i>	1.00	0.20	4.00	0.20	0.17	0.25	0.25	1.00	1.00	0.04
<i>Di</i>	1.00	0.17	4.00	0.25	0.17	0.20	0.25	1.00	1.00	0.03

Be basin elevation, *Sl* slope, *As* aspect, *Lg* lithology, *St* soil type, *Ld* lineament density, *Rr* relative relief, *Ri* ruggedness index, *Di* dissection index

Table 4 Pair-wise comparison matrix of seven selected parameters for preparing drainage diversity map

	<i>Fs</i>	<i>Dd</i>	<i>DI</i>	<i>Dt</i>	<i>Lo</i>	<i>Jf</i>	<i>In</i>	Weight
<i>Fs</i>	1.00	0.20	1.00	0.17	1.00	1.00	4.00	0.08
<i>Dd</i>	5.00	1.00	4.00	1.00	5.00	4.00	5.00	0.30
<i>DI</i>	1.00	0.25	1.00	0.20	1.00	1.00	5.00	0.09
<i>Dt</i>	6.00	1.00	5.00	1.00	5.00	5.00	5.00	0.34
<i>Lo</i>	1.00	0.20	1.00	0.20	1.00	1.00	1.00	0.07
<i>Jf</i>	1.00	0.25	1.00	0.20	1.00	1.00	2.00	0.07
<i>In</i>	0.25	0.20	0.20	0.20	1.00	0.50	1.00	0.04

Fs stream frequency, *DD* drainage density, *DI* drainage intensity, *DT* drainage texture, *LO* length of overland flow, *JF* junction frequency, *IN* infiltration number

ranked given to each sub-classes. The consistency ratio (CR) was defined as the ratio between the consistency index and the random consistency index (Mukherjee and Singh 2020). The inconsistency is permitted if the consistency ratio is less than or equal to 0.1, but if the consistency ratio is larger than 0.1, the subjective judgment must be revised. The CR is expressed as:

$$CR = \frac{CI}{RCI} \tag{8}$$

where, *RCI* = the random consistency index, and *CI* = consistency index, which can be expressed as follows:

$$CI = \frac{\lambda_{max} - n}{n - 1} \tag{9}$$

where, λ_{max} = the biggest particular value in the matrix, and $n - 1$ = the matrix’s order. The RCI value is depicted in Table 5 based on Saaty (1990). The CR is scaled from 0 to 1, where 1 indicates the chance of a randomly produced matrix and CR less than 0.10 indicates a reasonable level of homogeneity (Malczewski 2006). The resulting weights are shown in Table 6 with an acceptable CR. As the linear weighted combination computation rule, weights should add up to 1.0, i.e.,

$$\sum_{j=1}^n w_j = 1 \tag{10}$$

Validation of the work

Validation of the LSZ is required for the scientific significance and utility of the study. The final LSZ of the present study area has been validated through systematic validation processes. In the first step, validation is done by computing the frequency density of landslides with the landslide occurrences data of the GSI. In the second step, the final map is validated by preparing the ROC-AUC (Receiver Operating Characteristic-Area Under the Curve). This ROC-AUC has been prepared in ArcGIS software using the “ArcSDM” tool. It is a helpful tool used to validate the final susceptibility map of such kinds of studies. The landslide sample points used for validation are presented in the study area’s location map (Fig. 1). We used the historical landslide data of the studied region, which was collected from the Geological Survey of India (GSI). In the ROC, FPR (false positive rate) and TPR (true positive rate) have been calculated using Eqs. 11 and 12. The FPR denotes the proportion of incorrect predictions in the positive class,

and the TPR denotes the proportion of correct predictions in the positive class.

$$FPR = \frac{FP}{FP + TN} \tag{11}$$

$$TPR = \frac{TP}{TP + FN} \tag{12}$$

where FP is the total number of false positives, TN is the total number of true negatives, TP is the total number of true positives, and FN is the total number of false negatives.

Results

Relief diversity of the basin

The relief diversity (RD) represents the vulnerability of the study area based on terrain properties and slope instability (Basu and Pal 2019). It has been produced in respect of nine parameters, viz. “Be,” “Rr,” “Di,” “Ri,” “Sl,” “As,” “Lg,” “Ld,” and “St” of the basin. The produced map was categorized into five successive zones, i.e., “very low” (2.40%), “low” (34.02%), “moderate” (45.01%), “high” (18.01%), and “very high” (0.56%), as illustrated in Fig. 5a. In this vulnerability indicator, the “moderate” zone bears the highest area, while the “very high” zone bears the lowest area and is found in the southwestern part of the basin. Basically, in terms of the condition of the terrain, the “very high” relief diversity zone is most vulnerable, and the “very low” zone is least vulnerable, occupied in the lower section of the basin.

Drainage diversity of the basin

The drainage diversity (DD) of the basin is portrayed based on the strength of the properties of the drainages (Basu and Pal 2019). It results from the “Fs,” “Dd,” “Dt,” “DI,” “Lo,” “Jf,” and “In.” The spatial distribution of the DD is displayed in Fig. 5b, and it is also categorized into five classes, viz., “very low,” “low,” “moderate,” “high,” “very high.” The “very high” DD is mainly found in the upper part of the region, and it has been successively low towards the lower reaches. The “very high” zone is characterized by steep sloping land, high drainage density, high stream frequency, and vice-versa. The “low” DD zone occupies the maximum area (45.54%) of the basin, while the “very high” zone occupies the minimum extent (5.07%). The “moderate” DD zone covered 25.98% area, the

Table 5 Random consistency index (RCI) based on Saaty (1990)

<i>n</i>	1	2	3	4	5	6	7	8	9	10	11	12	13
RI	0	0	0.58	0.9	1.12	1.24	1.32	1.41	1.45	1.49	1.51	1.48	1.56

Table 6 Normalized weight for all parameters based on AHP and rank given to their sub-classes based on landslide vulnerability

Parameters	Classes	AHP normalized weights	Influence (%)	Rank of sub-classes based on Saaty's scale
Drainage diversity (DD) parameters				
Drainage density	1.84–3.34	0.306	30.6	1
	3.34–4.07			2
	4.07–4.74			3
	4.74–5.63			4
	5.63–7.15			5
Drainage texture	0–1	0.340	34.0	1
	1–2			2
	2–3			3
	3–4			4
	4–6			5
Drainage intensity	0.64–1.71	0.091	9.1	1
	1.71–2.17			2
	2.17–2.67			3
	2.67–3.71			4
	3.71–5.85			5
Infiltration number	7.59–31.26	0.043	4.3	1
	31.26–43.77			2
	43.77–63.87			3
	63.87–88.44			4
	88.44–121.04			5
Stream frequency	3–7	0.082	8.2	1
	7–9			2
	9–13			3
	13–16			4
	16–24			5
Length of overland flow	0.92–1.67	0.064	6.4	1
	1.67–2.03			2
	2.03–2.37			3
	2.37–2.81			4
	2.81–3.57			5
Junction frequency	0.00–2.59	0.074	7.4	1
	2.59–5.19			2
	5.19–7.79			3
	7.79–10.29			4
	10.39–12.99			5
Relief diversity (RD) parameters				
Basin elevation	230–722	0.032	3.2	1
	722–1086			2
	1086–1446			3
	1446–1820			4
	1820–2478			5
Soil type	Loamy skeletal	0.207	20.7	5
	Coarse loamy			2
Dissection index	0.05–0.21	0.034	3.4	1
	0.21–0.28			2
	0.28–0.34			3
	0.34–0.42			4
	0.42–0.58			5

Table 6 (continued)

Parameters	Classes	AHP normalized weights	Influence (%)	Rank of sub-classes based on Saaty’s scale
Ruggedness index	0.00–0.58	0.035	3.5	1
	0.58–1.13			2
	1.13–1.76			3
	1.76–2.46			4
	2.46–3.12			5
Relative relief	140–357	0.080	8.0	1
	357–443			2
	443–512			3
	512–601			4
	604–895			5
Aspect	Flat	0.018	1.8	2
	North			2
	Northeast			2
	East			2
	Southeast			2
	South			3
	Southwest			3
	West			2
	Northwest			2
	North			2
Slope	0.33–15.86	0.328	32.8	1
	15.86–23.27			2
	23.27–29.99			3
	29.99–37.87			4
	37.87–86.42			5
Lithology	Gorubathan	0.159	15.9	2
	Kanchenjunga gneiss			4
	Chungthang			3
Lineament density	0–0.28	0.107	10.7	1
	0.28–0.79			2
	0.79–1.21			3
	1.21–1.57			4
	1.57–1.83			5

“very low” DD zone covered 14.01% area, and the “high” DD zone covered 9.40% area of the region.

Landslide susceptibility zones

The landslide susceptibility mapping (LSM) of the Ragnu Khola River Basin was prepared using the AHP MCDM method based on 16 morphometric parameters. In this study, mainly LSM is related to the morphometric characteristics of the river. It represents the landslide susceptibility of the region in relation to relief and drainage conditions (Basu and Pal 2019). The LSM is displayed in Fig. 6 with five distinct zones. The zones are categorized using the natural break classification

technique to stratify the generated map into five susceptibility groups (Akgun et al. 2012; Jaafari et al. 2014; Achour et al. 2017; Moayedi et al. 2019a, b), viz. “very low,” “low,” “moderate,” “high,” and “very high.” The “moderate” susceptible zone contains most of the area (47.70%) of the region, followed by “low” zone (31.70%), “high” zone (17.83%), “very high” zone (1.45%), and “very low” zone (1.32%) (Fig. 7).

The spatial distribution pattern demonstrates that the occurrences of landslide phenomena have been decreasing from the higher elevated lands to the lower elevated lands of the basin, i.e., from the southwest to the northeast corner of the map. Therefore, the upper catchment is very highly susceptible to landslide hazards. The “very

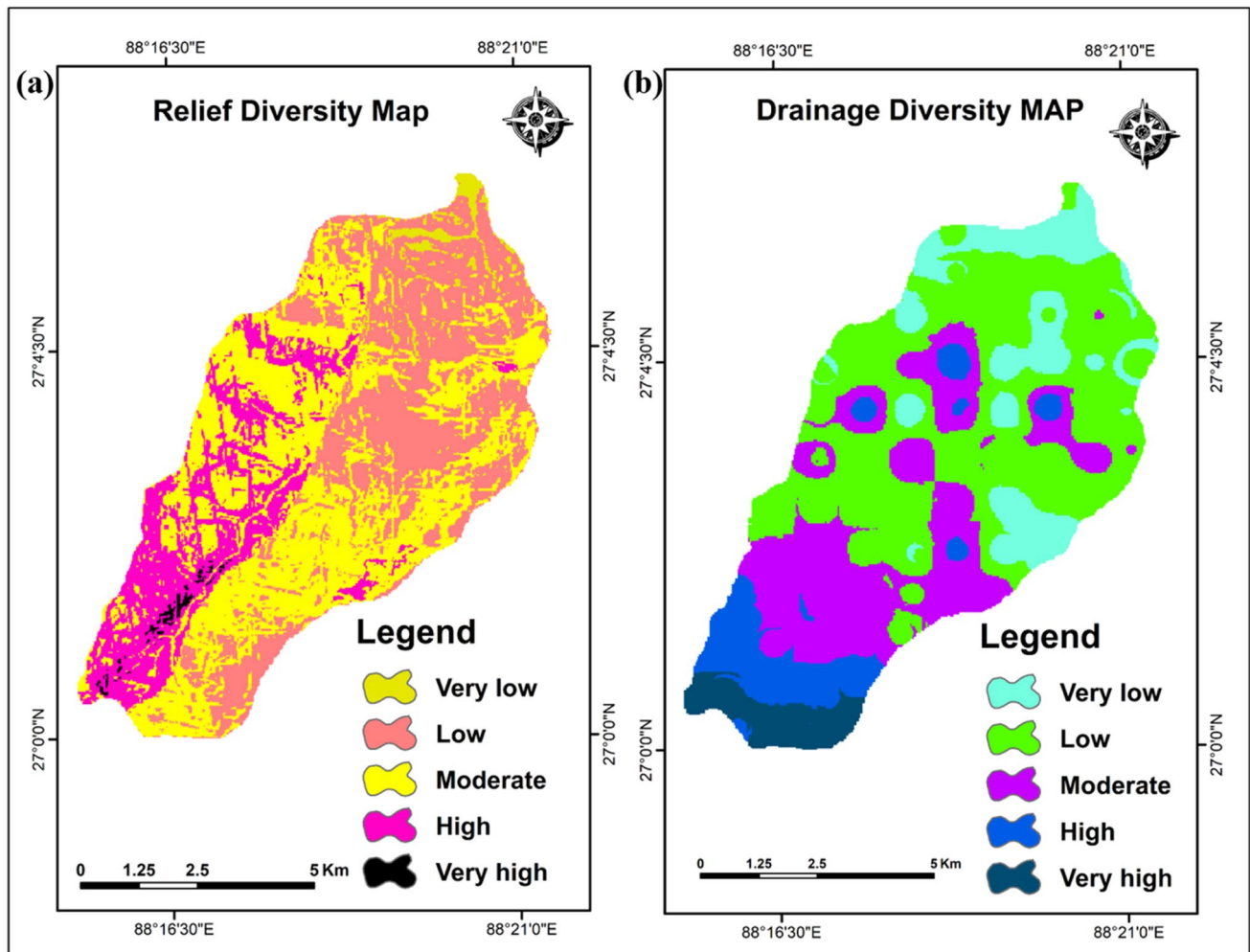


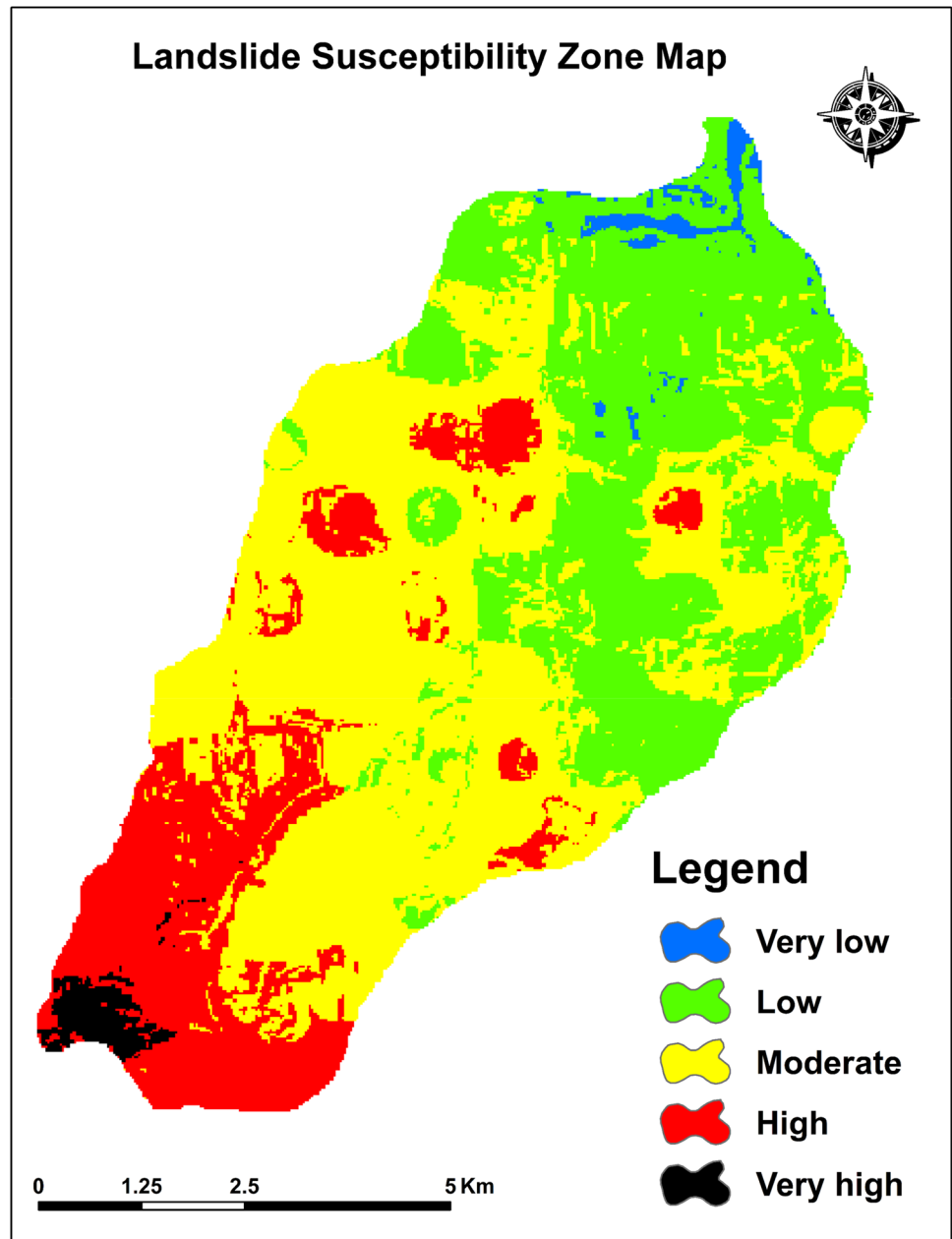
Fig. 5 **a** Relief diversity and **b** drainage diversity maps of the Ragnu Khola River Basin in the Darjeeling Himalaya

high” zone is associated with highly elevated land, bearing 1820 to 2478 m in height. The region is also represented by high “Dd” (5.63 to 7.15 km/km²), maximum “Jf” (10.39 to 12.99), and “Fs” (13 to 24 streams/km²), and highly rugged topography. Geologically, the zones ranging from “very high” to “moderate” landslide susceptibility are situated over the Kanchenjunga Gneiss formation and high lineament density zone (0.79 to 1.83 km/km²). The “high” susceptible areas are most vulnerable in terms of both DD and RD. Here, the rate of soil erosion is high due to extreme DD and RD, and the region is not suitable for agricultural and constructional activities (Pal and Saha 2017). The Chungthang and Gorubathan formation are less susceptible to landslides in the basin. The “low” and “very low” susceptible areas are less in terms of “Dd” (1.84 to 4.07 km/km²), ruggedness (0 to 1.13), and “Rr” (140 to 443 m). These zones are often found between 230 to 722 m altitudes, with “Ld” ranging from 0 to 0.28 km/km².

Validation

Based on the landslide occurrence data of the study area, the authors have computed the frequency density of landslides (FDL) (Basu and Pal 2019), as illustrated in Table 7. The “very high” (2.19/km²) FDL is associated with the “very high” LSZ. The “high” (0.80/km²) FDL area is also found for the “high” LSZ. In comparison, the “moderate” (0.36/km²) FDL actually falls in the “moderate” LSZ. “Very low” LSZ indicates no landslide point due to the FDL being zero. The second method entails creating a ROC for verification of the LSZ. The AUC achieved by the model is based on the landslide inventory map (Fig. 1c) and the produced landslide susceptibility map of the river basin. The outcome reveals 0.721, i.e., 72.10% area under the curve (AUC) (Fig. 8). The AUC value ranges from 0.60 to 1, where 0.60–0.70 show satisfactory, 0.70–0.80 show good, 0.80–0.90 show very good, and 0.90–1 show excellent outcome (Mitra and Roy 2022). The result of the study area implies a good accuracy rate as it

Fig. 6 Landslide susceptibility zones in the Ragnu Khola River Basin of Darjeeling Himalaya



falls between 0.70 to 0.80 (Rasyid et al. 2016). Therefore, all the morphometric indicators are acceptable in determining the landslide susceptibility model of the Ragnu Khola Basin. The google earth images of landslide-prone areas also manifest in Fig. 9, mainly dominating in the “high” to “very high” LSZ.

Discussion

In the Darjeeling Himalayas, landslides are the most frequent natural disaster, and they have been enlarging progressively (Chawla et al. 2018). It is an unavoidable natural disaster that directly threatens the economic and social progress of

Darjeeling Himalaya. Landslides can be triggered by natural as well as man-made activities such as rainstorms, earthquakes, deforestation, etc. It has a high death toll and causes significant damage to land and property (Ngo et al. 2021).

The landslide susceptibility areas of the Ragnu Khola River Basin in the Darjeeling Himalayan region were illustrated by integrated morphometric data and the GIS-based MCDM method throughout this study. It classified the river basin into five distinctive zones. Accuracy is typically calculated according to DeLong et al. (1988) by $(TP + TN)/(TP + TN + FP + FN)$. The accuracy level of the produced LSM is 72.10%. The research identified that about 20% area of the river basin was demarcated

Fig. 7 Area-wise distribution of landslide susceptibility zones in the Ragnu Khola River Basin

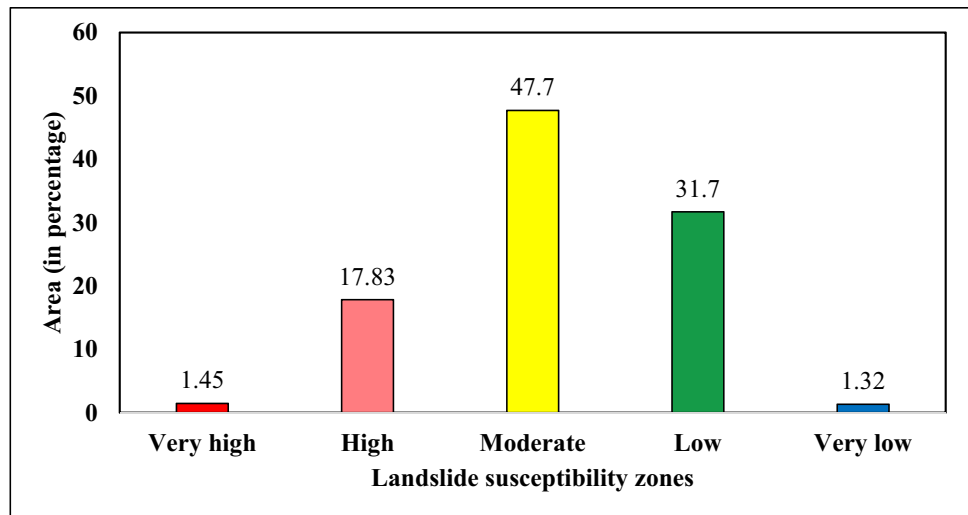
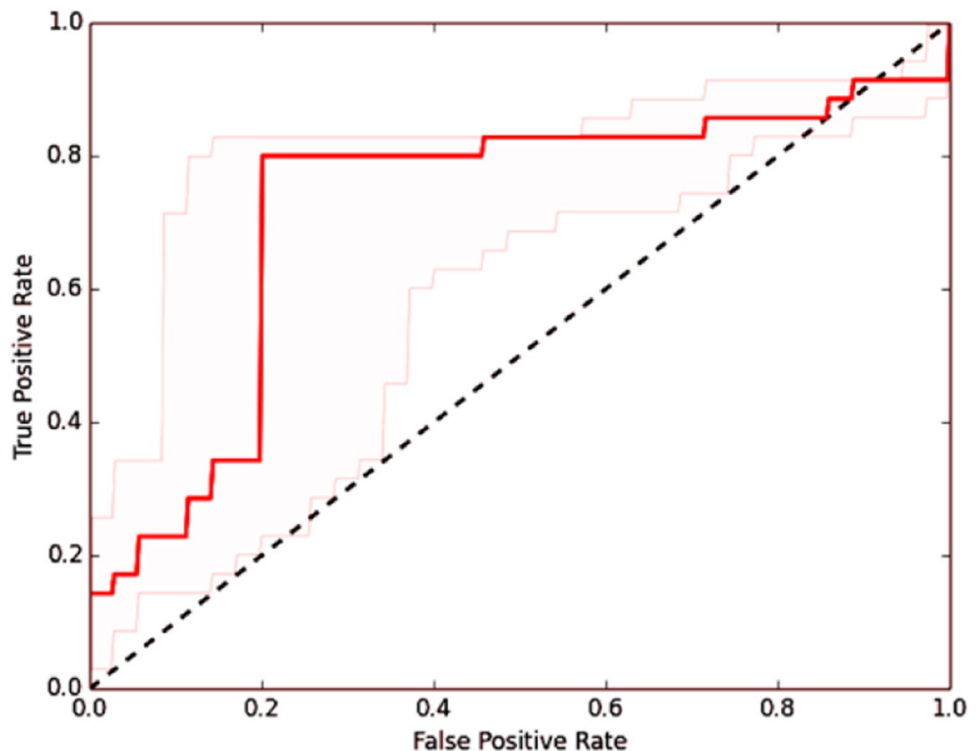


Table 7 Frequency density of landslide (FDL) occurrences in different landslide susceptibility zones

Landslide susceptibility zones	Area in km ²	Number of landslides	FDL (no./km ²)
Very high	0.90	2	2.19
High	11.50	9	0.80
Moderate	30.45	11	0.36
Low	20.28	6	0.29
Very low	0.90	0	0

in a highly landslide-prone zone, and about 50% area was demarcated in the moderate landslide-prone zone; therefore, the study area is considered very much susceptible to landslides in the Darjeeling Himalayan region. A similar kind of study in this region has been done by Basu and Pal (2018). They also demonstrated that 7.61% area of the Gish Basin was very much landslide susceptible with an 86.60% predicted rate. Several studies, viz., Bhattacharya (2013), Chawla et al. (2018), Chakraborty et al. (2018), Mandal and Mandal (2018),

Fig. 8 ROC curve for validation of the landslide susceptibility zones



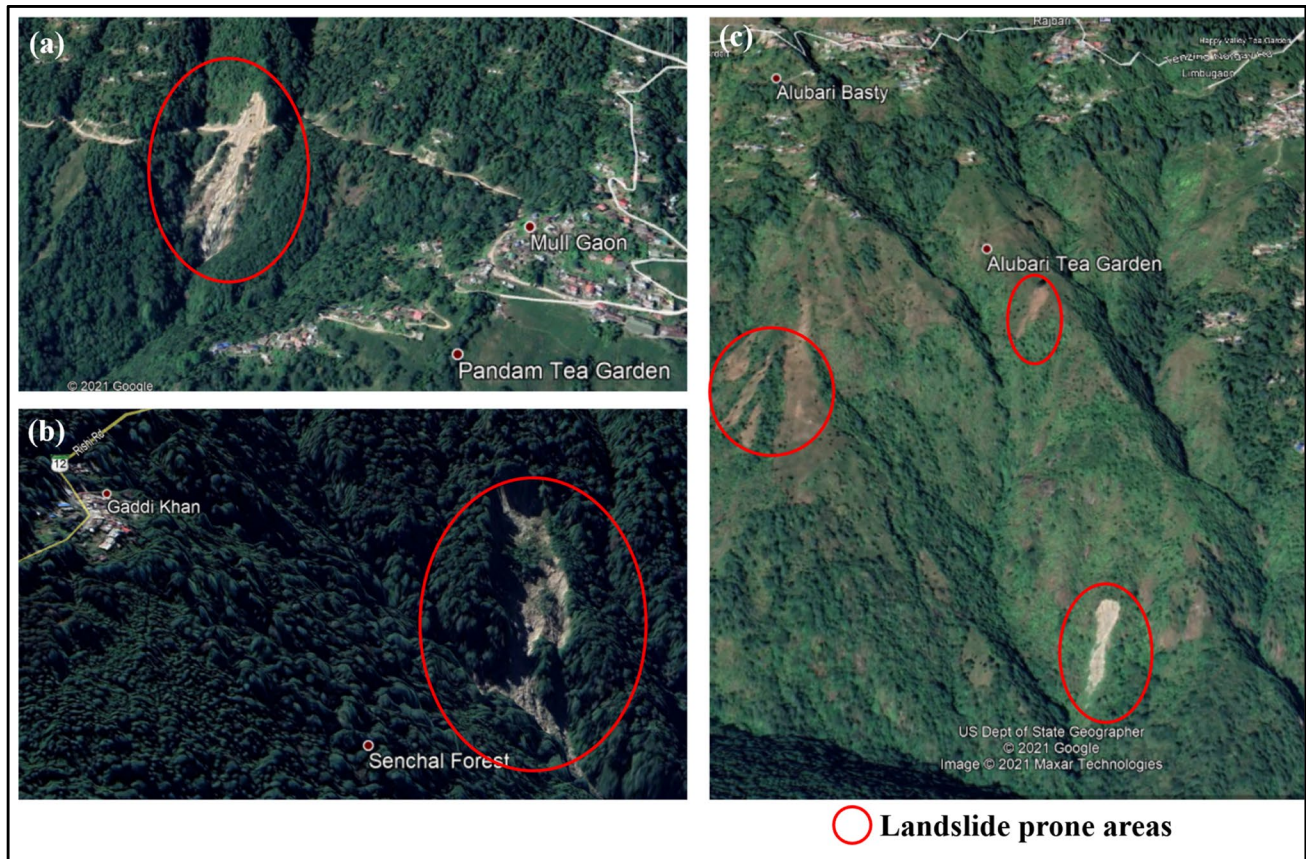


Fig. 9 Landslide scars in the Ragnu Khola River Basin in the Darjeeling Himalaya (location: **a** 27° 02' 00" N, 88° 16' 26" E; **b** 27° 00' 16" N, 88° 16' 39" E; and **c** 27° 01' 23" N, 88° 16' 04" E; 27° 01' 10" N, 88° 15' 58" E; 27° 01' 16" N, 88° 16' 17" E)

Das and Lepcha (2019), Saha and Saha (2021), and Das et al. (2022) also observed in the Darjeeling Himalayan region as it is very much frequent in the study area.

The study can be improved by comparative analysis of the landslide susceptibility maps of the river basin produced by different MCDM as well as machine learning methods. For the validation of landslide susceptibility mapping, ROC-AUC (Sameen et al. 2020; Lucchese et al. 2021a, b) is a popular method, but there are some other validation techniques like kappa index (Gautam et al. 2021), Information Gain Ratio (IGR), and some statistical inferences such as sensitivity, specificity, positive predictive value, negative predictive value, accuracy, etc. (Nhu et al. 2020), can be applied for landslide susceptibility mapping work (Afolayan et al. 2020). In spite of ROC-AUC, other statistical validation techniques like MAE (mean absolute error) and RMSE (root mean square error) can be applied for further study (Afolayan et al. 2020). The primary purpose of this investigation is to determine how the morphometry of a river basin impacts the landslides and their consequences and to recommend critical ways to reduce their severity in the Darjeeling

Himalaya. The findings of this study reveal that while landslides and their effects cannot be entirely eliminated, they can be reduced to less severe and less dangerous by taking only some simple precautions.

Landslide is a persistent threat to human life and livelihood in most parts of the world, particularly in hilly areas where population and economy have been rapidly expanded. So, some landslide preventive measures should be adopted to maintain the normality of hilly areas' population livelihood. There are some direct techniques for preventing landslides, such as modifying slope geometry, vegetation placement and management, using chemical agents to reinforce slope material, constructing rock buttresses and retaining walls, debris removal, diverting waste routes, and rerouting surface and underwater drainage (drainage pipes, ditches, berms, and catchment basins). In the study area, terrace cultivation needs to stop at the top of the hills because tillage and irrigation increase infiltration, which leads to more landslide events. Constructions are experiencing exponential growth in the studied region to satisfy the demands of the large population. In order to decrease the probability of a landslide,

construction work should be done scientifically. The southwestern part of the study area is less vegetated, and it is a significant factor in landslides. So, both the local community and the government agency should focus to checked deforestation and will need more tree plantations in this region.

Conclusions

The landslide susceptibility mapping (LSM) of the Ragnu Khola River Basin in Darjeeling Himalaya included a variety of morphometric criteria, and these criteria were also divided into two-part, such as drainage diversity (DD) and relief diversity (RD) indicators. These morphometric parameters reflect the characteristics of the hydro-geomorphological system of the study area. It was observed during the study that morphometric parameters are capable of creating the landslide susceptibility map. The study region is only about 64.79 km² in its extent, and the morphometric variables are reliable even in this small-scale perspective for identifying landslide susceptibility zones (LSZ). Aside from that, morphometric parameters show that areas with higher drainage density and cliffs are primarily susceptible to landslide phenomena in the river basin. Almost monsoon rains cause landslides in these places every year. The resulting map has provided the spatial distribution of landslide zones, and the FDL and ROC curve analysis validated it. It came out from the study that a high LSZ is interrelated to the places particularly vulnerable to drainage and relief conditions. The upper catchment of the basin is very sensitive and varies from high to very high landslide zones, while the lower part is less vulnerable. There, 17.83% area is highly susceptible to landslides, which are observed in the upper catchment of the basin. Therefore, there should be implemented restrictions and proper guidelines for constructional activity. Thus, the MCDM technique is useful globally to generate such a kind of susceptibility map. The work will also assist the decision-makers in developing strategies to prevent landslide destruction. This type of work will be required in the future for appropriate planning of developmental activities in tectonically active areas.

Declarations

Conflict of interest The authors declare no competing interests.

References

- Achour Y, Boumezbeur A, Hadji R, Chouabbi A, Cavaleiro V, Bendaoud EA (2017) Landslide susceptibility mapping using analytic hierarchy process and information value methods along a highway road section in Constantine. *Algeria Arabian J Geosci* 10(8):194. <https://doi.org/10.1007/s12517-017-2980-6>
- Afolayan AH, Ojokoh BA, Adetunmbi AO (2020) Performance analysis of fuzzy analytic hierarchy process multi-criteria decision support models for contractor selection. *Scientific African* 9:e00471. <https://doi.org/10.1016/j.sciaf.2020.e00471>
- Agarwal CS (1998) Study of drainage pattern through aerial data in Naugarh area of Varanasi district, UP. *J Indian Soc Remote Sens* 26(4):169–175. <https://doi.org/10.1007/BF02990795>
- Ahmadlou M, Karimi M, Alizadeh S, Shirzadi A, Parvinnejhad D, Shahabi H, Panahi M (2019) Flood susceptibility assessment using integration of adaptive network-based fuzzy inference system (ANFIS) and biogeography-based optimization (BBO) and BAT algorithms (BA). *Geocarto Int* 34(11):1252–1272. <https://doi.org/10.1080/10106049.2018.1474276>
- Akgun A, Sezer EA, Nefeslioglu HA, Gokceoglu C, Pradhan B (2012) An easy-to-use MATLAB program (MamLand) for the assessment of landslide susceptibility using a Mamdani fuzzy algorithm. *Comput Geosci* 38(1):23–34. <https://doi.org/10.1016/j.cageo.2011.04.012>
- Alano E, Lee M (2016). Natural disaster shocks and macroeconomic growth in Asia: evidence for typhoons and droughts. *Asian Dev Bank Econ Working Paper Series*, (503).
- Altın TB, Gökçaya E (2018) Assessment of landslide-triggering factors and occurrence using morphometric parameters in Geyraz Basin, Tokat. *Northern Turkey Environ Earth Sci* 77(4):1–20. <https://doi.org/10.1007/s12665-018-7315-8>
- Arabameri A, Pourghasemi HR, Yamani M (2017) Applying different scenarios for landslide spatial modeling using computational intelligence methods. *Environ Earth Sci* 76(24):1–20. <https://doi.org/10.1007/s12665-017-7177-5>
- Arabameri A, Pradhan B, Rezaei K, Sohrabi M, Kalantari Z (2019) GIS-based landslide susceptibility mapping using numerical risk factor bivariate model and its ensemble with linear multivariate regression and boosted regression tree algorithms. *J Mt Sci* 16(3):595–618. <https://doi.org/10.1007/s11629-018-5168-y>
- Ayalew L, Yamagishi H (2005) The application of GIS-based logistic regression for landslide susceptibility mapping in the Kakuda-Yahiko Mountains. *Central Japan Geomorphol* 65(1–2):15–31. <https://doi.org/10.1016/j.geomorph.2004.06.010>
- Bahrami Y, Hassani H, Maghsoudi A (2021) Landslide susceptibility mapping using AHP and fuzzy methods in the Gilan province. *Iran Geojournal* 86(4):1797–1816. <https://doi.org/10.1007/s10708-020-10162-y>
- Basu T, Pal S (2018) Identification of landslide susceptibility zones in Gish River basin, West Bengal, India. *Georisk Assess Manag Risk for Eng Syst Geohaz* 12(1):14–28. <https://doi.org/10.1080/17499518.2017.1343482>
- Basu T, Pal S, (2019) RS-GIS based morphometrical and geological multi-criteria approach to the landslide susceptibility mapping in Gish River Basin, West Bengal. *India Adv Space Res* 63(3):1253–1269. <https://doi.org/10.1016/j.asr.2018.10.033>
- Bennie J, Hill MO, Baxter R, Huntley B (2006) Influence of slope and aspect on long-term vegetation change in British chalk grasslands. *J Ecol* 94(2):355–368. <https://doi.org/10.1111/j.1365-2745.2006.01104.x>
- Beullens J, Van de Velde D, Nyssen J (2014) Impact of slope aspect on hydrological rainfall and on the magnitude of rill erosion in Belgium and northern France. *CATENA* 114:129–139. <https://doi.org/10.1016/j.catena.2013.10.016>
- Bhattacharya SK (2013) The study of Paglajhora landslide in the Darjeeling Hills, West Bengal. *India Ind J Spat Sci* 4.0(1):21–27
- Chakraborty K, Mitra R, Saha S, Mandal DK (2018) Identification of landslide prone areas in Tista catchment through landslide susceptibility mapping, West Bengal. In: Sarkar S (ed) *Disaster management in Sub-Himalayan North Bengal*. UGC-SAP DRS-II, Monograph, pp 1–11

- Chamling M (2013) Landslides: a geographical review in and around Pagla Jhora Region of the Eastern Himalayan belt of Darjeeling. West Bengal, Peripex-Ind Res 2(8):131–133
- Chawla A, Chawla S, Pasupuleti S, Rao ACS, Sarkar K, Dwivedi R (2018) Landslide susceptibility mapping in Darjeeling Himalayas. *Advances in Civil Engineering, India*. <https://doi.org/10.1155/2018/6416492>
- Chen W, Xie X, Wang J, Pradhan B, Hong H, Bui DT, Duan Z, Ma J (2017) A comparative study of logistic model tree, random forest, and classification and regression tree models for spatial prediction of landslide susceptibility. *CATENA* 151:147–160. <https://doi.org/10.1016/j.catena.2016.11.032>
- Chen W, Shahabi H, Shirzadi A, Hong H, Akgun A, Tian Y, Liu J, Zhu AX, Li S (2019) Novel hybrid artificial intelligence approach of bivariate statistical-methods-based kernel logistic regression classifier for landslide susceptibility modeling. *Bull Eng Geol Env* 78(6):4397–4419. <https://doi.org/10.1007/s10064-018-1401-8>
- Chu L, Wang LJ, Jiang J, Liu X, Sawada K, Zhang J (2019) Comparison of landslide susceptibility maps using random forest and multivariate adaptive regression spline models in combination with catchment map units. *Geosci J* 23(2):341–355. <https://doi.org/10.1007/s12303-018-0038-8>
- Clarke JI (1996) Morphometry from maps. *Essays in geomorphology CLIMATE-DATA.ORG* 2021. Retrieved from: <https://weather-and-climate.com/average-monthly-Rainfall-Temperature-Sunshine,darjeeling,India>.
- Crawford MM, Dortch JM, Koch HJ, Killen AA, Zhu J, Zhu Y, Bryson LS, Haneberg WC (2021). Using landslide-inventory mapping for a combined bagged-trees and logistic-regression approach to determining landslide susceptibility in eastern Kentucky, United States. *Quarterly Journal of Engineering Geology and Hydrogeology*. <https://doi.org/10.1144/qjegh2020-177>.
- Das G, Lepcha K (2019) Application of logistic regression (LR) and frequency ratio (FR) models for landslide susceptibility mapping in Relli Khola river basin of Darjeeling Himalaya. *India SN Appl Sci* 1(11):1–22. <https://doi.org/10.1007/s42452-019-1499-8>
- Das S, Sarkar S, Kanungo DP (2022) GIS-based landslide susceptibility zonation mapping using the analytic hierarchy process (AHP) method in parts of Kalimpong Region of Darjeeling Himalaya. *Environ Monit Assess* 194(3):1–28. <https://doi.org/10.1007/s10661-022-09851-7>
- DeLong ER, DeLong DM, Clarke-Pearson DL (1988) Comparing the areas under two or more correlated receiver operating characteristic curves: a nonparametric approach. *Biometrics*, 837–845
- District Survey Report, Darjeeling (2021), Retrieved from: <https://weather-and-climate.com/average-monthly-Rainfall-Temperature-Sunshine,darjeeling,India>.
- Dou J, Yamagishi H, Zhu Z, Yunus AP, Chen CW (2018) TXT-tool 1.081–6.1 A comparative study of the binary logistic regression (BLR) and artificial neural network (ANN) models for GIS-based spatial predicting landslides at a regional scale. In *Landslide dynamics: ISDR-ICL landslide interactive teaching tools* (139–151). Springer, Cham. https://doi.org/10.1007/978-3-319-57774-6_10.
- Erener A, Düzgün HSB (2010) Improvement of statistical landslide susceptibility mapping by using spatial and global regression methods in the case of More and Romsdal (Norway). *Landslides* 7(1):55–68. <https://doi.org/10.1007/s10346-009-0188-x>
- Faniran A (1968) The index of drainage intensity: a provisional new drainage factor. *Aust J Sci* 31(9):326–330
- Gautam P, Kubota T, Sapkota LM, Shinohara Y (2021) Landslide susceptibility mapping with GIS in high mountain area of Nepal: a comparison of four methods. *Environ Earth Sci* 80(9):1–18. <https://doi.org/10.1007/s12665-021-09650-2>
- Gayen S, Bhunia GS, Shit PK (2013) Morphometric analysis of Kangshabati-Darakeswar Interfluvies area in West Bengal, India using ASTER DEM and GIS techniques. *J Geol Geosci* 2(4):1–10. <https://doi.org/10.4172/2329-6755.1000133>
- Gorokhovich Y, Vustianiuk A (2021) Implications of slope aspect for landslide risk assessment: a case study of Hurricane Maria in Puerto Rico in 2017. *Geomorphology*, 107874. <https://doi.org/10.1016/j.geomorph.2021.107874>.
- Gu T, Li J, Wang M, Duan P (2021) Landslide susceptibility assessment in Zhenxiong County of China based on geographically weighted logistic regression model. *Geocarto International*, 1–23. <https://doi.org/10.1080/10106049.2021.1903571>.
- Hasegawa S, Nonomura A, Nakai S DRK (2014) Drainage density as rainfall induced landslides susceptibility index in small catchment area. *Int J Landslide Environ* 1(1):27–28
- Hong H, Panahi M, Shirzadi A, Ma T, Liu J, Zhu AX, Chen W, Kougias I, Kazakis N (2018) Flood susceptibility assessment in Hengfeng area coupling adaptive neuro-fuzzy inference system with genetic algorithm and differential evolution. *Sci Total Environ* 621:1124–1141. <https://doi.org/10.1016/j.scitotenv.2017.10.114>
- Horton RE (1932) Drainage-basin characteristics. *EOS Trans Am Geophys Union* 13(1):350–361. <https://doi.org/10.1029/TR013i001p00350>
- Horton RE (1945) Erosional development of streams and their drainage basins; hydrophysical approach to quantitative morphology. *Bull Geol Soc Am* 56:275–370
- Hurtrez JE, Sol C, Lucazeau F (1999) Effect of drainage area on hypsometry from an analysis of small-scale drainage basins in the Siwalik Hills (Central Nepal). *Earth Surf Proc Landforms: J British Geomorphol Res Group* 24(9):799–808. [https://doi.org/10.1002/\(SICI\)1096-9837\(199908\)24:9%3c799::AID-ESP12%3e3.0.CO;2-4](https://doi.org/10.1002/(SICI)1096-9837(199908)24:9%3c799::AID-ESP12%3e3.0.CO;2-4)
- Iqbal J, Peng C, Hussain ML, Pourghasemi HR, De-Qiang C, Shah SU, Pradhan B (2021) Landslide susceptibility assessment along the dubairdudishal section of the Karakoram highway, northwestern Himalayas. *Pakistan Acta Geodyn Geomater* 18(2):137–155. <https://doi.org/10.13168/AGG.2021.0010>
- Islam MR, Khan NA (2018) Threats, vulnerability, resilience and displacement among the climate change and natural disaster-affected people in South-East Asia: an overview. *J Asia Pacific Econ* 23(2):297–323
- Jaafari A, Najafi A, Pourghasemi HR, Rezaeian J, Sattarian A (2014) GIS-based frequency ratio and index of entropy models for landslide susceptibility assessment in the Caspian forest, northern Iran. *Int J Environ Sci Technol* 11(4):909–926. <https://doi.org/10.1007/s13762-013-0464-0>
- Jacynth Jennifer J, Saravanan S (2021) Artificial neural network and sensitivity analysis in the landslide susceptibility mapping of Idukki district, India. *Geocarto International*, 1–23. <https://doi.org/10.1080/10106049.2021.1923831>.
- Kale VS, Gupta A (2001) Introduction to geomorphology. Orient Blackswan Private Limited
- Kaur L, Rishi MS, Singh G, Thakur SN (2020) Groundwater potential assessment of an alluvial aquifer in Yamuna sub-basin (Panipat region) using remote sensing and GIS techniques in conjunction with analytical hierarchy process (AHP) and catastrophe theory (CT). *Ecol Ind* 110:105850. <https://doi.org/10.1016/j.ecolind.2019.105850>
- Kaur H, Gupta S, Parkash S, Thapa R (2018) Knowledge-driven method: a tool for landslide susceptibility zonation (LSZ). *Geol Ecol Landscapes*, 1–15. <https://doi.org/10.1080/24749508.2018.1558024>.
- Keefer DK, Larsen MC (2007) Assessing landslide hazards. *Science*, 1136–1138.
- Liu Z, Gilbert G, Cepeda JM, Lysdahl AOK, Piciullo L, Hefre H LS (2021) Modelling of shallow landslides with machine learning

- algorithms. *Geosci Front* 12(1):385–393. <https://doi.org/10.1016/j.gsf.2020.04.014>
- Lucchese LV, de Oliveira GG, Pedrollo OC (2021a) Mamdani fuzzy inference systems and artificial neural networks for landslide susceptibility mapping. *Nat Hazards* 106(3):2381–2405
- Lucchese LV, de Oliveira GG, Pedrollo OC (2021b) Investigation of the influence of nonoccurrence sampling on landslide susceptibility assessment using Artificial Neural Networks. *CATENA* 198:105067. <https://doi.org/10.1016/j.catena.2020.105067>
- Luo Y, He SM, Chen FZ, Li XP, He JC (2015) A physical model considered the effect of overland water flow on rainfall-induced shallow landslides. *Geoenviron Dis* 2(1):1–11. <https://doi.org/10.1186/s40677-015-0017-6>
- Malczewski J (2006) GIS-based multi-criteria decision analysis: a survey of the literature. *Int J Geogr Inf Sci* 20(7):703–726. <https://doi.org/10.1080/13658810600661508>
- Manaouch M, Mohamed S, Imad F (2021) Coupling fuzzy logic and analytical hierarchy process (FAHP) with GIS for landslide susceptibility mapping (LSM) in Ziz upper watershed. SE Morocco
- Mandal S, Maiti R (2014) Role of lithological composition and lineaments in landsliding: a case study of Shivkhola Watershed, Darjeeling Himalaya. *Int J Geol Earth Environ Sci* 4(1):126–132
- Mandal B, Mandal S (2018) Analytical hierarchy process (AHP) based landslide susceptibility mapping of Lish River basin of eastern Darjeeling Himalaya. *India Adv Space Res* 62(11):3114–3132. <https://doi.org/10.1007/s12518-018-0248-9>
- Mehrabi M, Moayedi H (2021) Landslide susceptibility mapping using artificial neural network tuned by metaheuristic algorithms. *Environ Earth Sci* 80(24):1–20. <https://doi.org/10.1007/s12665-021-10098-7>
- Mehrabi M (2021) Landslide susceptibility zonation using statistical and machine learning approaches in Northern Lecco, Italy. *Natural Hazards*, 1–37. <https://doi.org/10.1007/s11069-021-05083-z>
- Mitra R, Roy D (2022) Delineation of groundwater potential zones through the integration of remote sensing, geographic information system, and multi-criteria decision-making technique in the sub-Himalayan foothills region, India. *Int J Energy Water Res* 1–21. <https://doi.org/10.1007/s42108-022-00181-5>
- Moayedi H, Mehrabi M, Kalantar B, AbdullahiMuazu MA, Rashid AS, Foong LK, Nguyen H (2019) Novel hybrids of adaptive neuro-fuzzy inference system (ANFIS) with several metaheuristic algorithms for spatial susceptibility assessment of seismic-induced landslide. *Geomatics Nat Hazards Risk* 10(1):1879–1911. <https://doi.org/10.1080/19475705.2019.1650126>
- Moayedi H, Mehrabi M, Mosallanezhad M, Rashid ASA, Pradhan B (2019b) Modification of landslide susceptibility mapping using optimized PSO-ANN technique. *Eng Comp* 35(3):967–984. <https://doi.org/10.1007/s00366-018-0644-0>
- Mondal S, Mandal S (2019) Landslide susceptibility mapping of Darjeeling Himalaya, India using index of entropy (IOE) model. *Appl Geomatics* 11(2):129–146. <https://doi.org/10.1007/s12518-018-0248-9>
- Mukherjee I, Singh UK (2020) Delineation of groundwater potential zones in a drought-prone semi-arid region of east India using GIS and analytical hierarchical process techniques. *Catena* 194:104681. <https://doi.org/10.1016/j.catena.2020.104681>
- Nad C (2015) Landslide hazard management of Darjeeling Hill—a critical need for inhabited. *Int J Hum Soc Sci Invention* 4(3):48–60
- Nadim F, Kjekstad O (2009) Assessment of global high-risk landslide disaster hotspots. In *Landslides—disaster risk reduction* (pp. 213–221). Springer, Berlin, Heidelberg. https://doi.org/10.1007/978-3-540-69970-5_11
- Nanehkaran YA, Mao Y, Azarafza M, Kockar MK, Zhu HH (2021) Fuzzy-based multiple decision method for landslide susceptibility and hazard assessment: a case study of Tabriz. Iran. *Geomech Eng* 24(5):407–418. <https://doi.org/10.12989/gae.2021.24.5.407>
- Navarro IJ, Yepes V, Martí JV (2019) A review of multi-criteria assessment techniques applied to sustainable infrastructure design. *Advances in civil engineering*, 2019 <https://doi.org/10.1155/2019/6134803>
- Ngo TQ, Dam ND, Al-Ansari N, Amiri M, Phong TV, Prakash I, Pham BT (2021) Landslide susceptibility mapping using single machine learning models: a case study from Pithoragarh District, India. *Advances in civil engineering*, 2021 <https://doi.org/10.1155/2021/9934732>
- Nhu VH, Shirzadi A, Shahabi H, Chen W, Clague JJ, Geertsema M, Jaafari A, Avand M, Miraki S, Talebpour Asl D, Pham BT (2020) Shallow landslide susceptibility mapping by random forest base classifier and its ensembles in a semi-arid region of Iran. *Forests* 11(4):421. <https://doi.org/10.3390/f11040421>
- Nir D (1957) The ratio of relative and absolute altitudes of Mt Carmel: a contribution to the problem of relief analysis and relief classification. *Geographical Review* 47(4):564–569
- Pal S, Saha TK (2017) Exploring drainage/relief-scape sub-units in Atrayee river basin of India and Bangladesh. *Spat Inf Res* 25(5):685–692. <https://doi.org/10.1007/s41324-017-0133-3>
- Patton PC, Baker VR (1976) Morphometry and floods in small drainage basins subject to diverse hydrogeomorphic controls. *Water Resour Res* 12(5):941–952. <https://doi.org/10.1029/WR012i005p00941>
- Petley D (2012) Global patterns of loss of life from landslides. *Geology* 40(10):927–930. <https://doi.org/10.1130/G33217.1>
- Pham QB, Achour Y, Ali SA, Parvin F, Vojtek M, Vojteková J, Al-Ansari N, Achu AL, Costache R, Khedher KM, Anh DT (2021) A comparison among fuzzy multi-criteria decision making, bivariate, multivariate and machine learning models in landslide susceptibility mapping. *Geomat Nat Haz Risk* 12(1):1741–1777. <https://doi.org/10.1080/19475705.2021.1944330>
- Pourghasemi HR, Mohammady M, Pradhan B (2012a) Landslide susceptibility mapping using index of entropy and conditional probability models in GIS: Safarood Basin. *Iran Catena* 97:71–84. <https://doi.org/10.1016/j.catena.2012.05.005>
- Pourghasemi HR, Pradhan B, Gokceoglu C (2012b) Application of fuzzy logic and analytical hierarchy process (AHP) to landslide susceptibility mapping at Haraz watershed. *Iran Natural Hazards* 63(2):965–996. <https://doi.org/10.1007/s11069-012-0217-2>
- Rasyid AR, Bhandary NP, Yatabe R (2016) Performance of frequency ratio and logistic regression model in creating GIS based landslides susceptibility map at Lompobattang Mountain. *Indonesia Geoenviron Dis* 3(1):1–16. <https://doi.org/10.1186/s40677-016-0053-x>
- Reddy GPO, Maji AK, Gajbhiye KS (2004) Drainage morphometry and its influence on landform characteristics in a basaltic terrain, Central India—a remote sensing and GIS approach. *Int J Appl Earth Obs Geoinf* 6(1):1–16. <https://doi.org/10.1016/j.jag.2004.06.003>
- Saaty TL (1990) An exposition of the AHP in reply to the paper “remarks on the analytic hierarchy process.” *Manage Sci* 36(3):259–268. <https://doi.org/10.1287/mnsc.36.3.259>
- Saaty TL (2004) Fundamentals of the analytic network process—multiple networks with benefits, costs, opportunities and risks. *J Syst Sci Syst Eng* 13(3):348–379. <https://doi.org/10.1007/s11518-006-0171-1>
- Saaty TL (2005) Analytic hierarchy process. *Encyclopedia of biostatistics*
- Saaty TL (2008) Decision making with the analytic hierarchy process. *Int J Services Sci* 1(1):83–98
- Saha A, Saha S (2021) Application of statistical probabilistic methods in landslide susceptibility assessment in Kurseong and its surrounding area of Darjeeling Himalayan, India: RS-GIS approach. *Environ Dev Sustain* 23(3):4453–4483. <https://doi.org/10.1007/s10668-020-00783-1>
- Saha AK, Gupta RP, Arora MK (2002) GIS-based landslide hazard zonation in the Bhagirathi (Ganga) valley. *Himalayas Int*

- J Remote Sens 23(2):357–369. <https://doi.org/10.1080/0143160010014260>
- Sahana M, Sajjad H (2017) Evaluating effectiveness of frequency ratio, fuzzy logic and logistic regression models in assessing landslide susceptibility: a case from Rudraprayag district. *India J Mountain Sci* 14(11):2150–2167. <https://doi.org/10.1007/s11629-017-4404-1>
- Saleem N, Huq M, Twumasi NYD, JavedA SA (2019) Parameters derived from and/or used with digital elevation models (DEMs) for landslide susceptibility mapping and landslide risk assessment: a review. *ISPRS Int J Geo Inf* 8(12):545. <https://doi.org/10.3390/ijgi8120545>
- Sameen MI, Pradhan B, Lee S (2020) Application of convolutional neural networks featuring Bayesian optimization for landslide susceptibility assessment. *CATENA* 186:104249. <https://doi.org/10.1016/j.catena.2019.104249>
- Sarkar S, Kanungo DP, Mehrotra GS (1995) Landslide hazard zonation: a case study in Garhwal Himalaya, India. *Mountain Research and Development*, 301–309.
- Sarkar S, Kanungo DP (2004) An integrated approach for landslide susceptibility mapping using remote sensing and GIS. *Photogrammetric Eng Remote Sens* 70(5):617–625. <https://doi.org/10.14358/PERS.70.5.617>
- Schumm SA (1956) Evolution of drainage systems and slopes in badlands at Perth Amboy, New Jersey. *Geol Soc Am Bull* 67(5):597–646. [https://doi.org/10.1130/0016-7606\(1956\)67\[597:EODSAS\]2.0.CO;2](https://doi.org/10.1130/0016-7606(1956)67[597:EODSAS]2.0.CO;2)
- Sharma LP, Patel N, Debnath P, Ghose MK (2012) Assessing landslide vulnerability from soil characteristics—a GIS-based analysis. *Arab J Geosci* 5(4):789–796. <https://doi.org/10.1007/s12517-010-0272-5>
- Shirzadi A, Shahabi H, Chapi K, Bui DT, Pham BT, Shahedi K, Ahmad BB (2017) A comparative study between popular statistical and machine learning methods for simulating volume of landslides. *CATENA* 157:213–226. <https://doi.org/10.1016/j.catena.2017.05.016>
- Smith GH (1935) The relative relief of Ohio. *Geogr Rev* 25(2):272–284
- Strahler AN (1952) Hypsometric (area-altitude) analysis of erosional topography. *Geol Soc Am Bull* 63(11):1117–1142. [https://doi.org/10.1130/0016-7606\(1952\)63\[1117:HAAOET\]2.0.CO;2](https://doi.org/10.1130/0016-7606(1952)63[1117:HAAOET]2.0.CO;2)
- Strahler AN (1956) Quantitative slope analysis. *Geol Soc Am Bull* 67(5):571–596. [https://doi.org/10.1130/0016-7606\(1956\)67\[571:QSA\]2.0.CO;2](https://doi.org/10.1130/0016-7606(1956)67[571:QSA]2.0.CO;2)
- Strahler AN (1964) Part II Quantitative geomorphology of drainage basins and channel networks. McGraw-Hill, New York, *Handbook of Applied Hydrology*, pp 4–39
- Sujatha ER, Sridhar V (2021) Landslide susceptibility analysis: a logistic regression model case study in Coonoor. *India Hydrology* 8(1):41. <https://doi.org/10.3390/hydrology8010041>
- Varnes DJ (1984) Landslide hazard zonation: a review of principles and practice. UNESCO, Paris, pp 1–63
- Virdi NS, Sah MP, Bartarya SK (1997) Mass wasting, its manifestations, causes and control: some case histories from Himachal Himalaya Perspectives of mountain risk engineering in the Himalayan Region. Gyanodaya Prakashan, Nainital, pp 111–130
- Wang G, Lei X, Chen W, Shahabi H, Shirzadi A (2020) Hybrid computational intelligence methods for landslide susceptibility mapping. *Symmetry* 12(3):325. <https://doi.org/10.3390/sym12030325>
- White GF (1974) Natural hazards, local, national, global. Oxford University Press
- Zarei E, Ramavandi B, Darabi AH, Omidvar M (2021) A framework for resilience assessment in process systems using a fuzzy hybrid MCDM model. *J Loss Prev Process Ind* 69:104375. <https://doi.org/10.1016/j.jlp.2020.104375>
- Zavoianca I (1985) Morphometry of drainage basins (development in water science). Publisher: Elsevier science, 20, 104–105.
- Zhou S, Zhang Y, Tan X, Abbas SM (2021) A comparative study of the bivariate, multivariate and machine-learning-based statistical models for landslide susceptibility mapping in a seismic-prone region in China. *Arab J Geosci* 14(6):1–19. <https://doi.org/10.1007/s12517-021-06630-5>

Springer Nature or its licensor holds exclusive rights to this article under a publishing agreement with the author(s) or other rightsholder(s); author self-archiving of the accepted manuscript version of this article is solely governed by the terms of such publishing agreement and applicable law.